

Herschel observations of planetary nebulae in the MESS program

First detection of OH⁺ emission in a planetary nebula



P.A.M. van Hoof¹, M. Etzaluze², G.C. Van de Steene¹, J. Cernicharo², K.M. Exter³, J.R. Goicoechea², M.J. Barlow⁴, B.M. Swinyard^{5,4}, T. Ueta⁶, T.L. Lim⁵, M.A.T. Groenewegen¹, E.T. Polehampton^{5,7}, and the MESS consortium

¹Royal Observatory of Belgium, Ringlaan 3, B-1180 Brussels, Belgium, ²Departamento de astrofísica, Centro de Astrobiología, CSIC-INTA. Torrejón de Ardoz, 28850 Madrid, Spain
³Instituut voor Sterrenkunde, Katholieke Universiteit Leuven, Celestijnenlaan 200 D, B-3001 Leuven, Belgium, ⁴Dept. of Physics & Astronomy, University College London, Gower St, London WC1E 6BT, UK, ⁵Space Science and Technology Department, Rutherford Appleton Laboratory, Oxfordshire, OX11 0QX, UK ⁶Dept. Of Physics and Astronomy, University of Denver, Mail Stop 6900, Denver, CO 80208, USA ⁷Dept. of Physics, University of Lethbridge, Lethbridge, Alberta, T1J 1B1, Canada

1. Introduction

The Herschel Guaranteed Time Key Project MESS (Mass loss of Evolved StarS; Groenewegen et al. 2011) brings together an international consortium of astrophysicists that observe a wide variety of evolved stellar objects in spectroscopic and photometric mode in the far-IR using both the PACS and SPIRE instruments on board the Herschel satellite. The main aims of this project are three-fold:

1. To study the time-dependence of the mass loss process, via a search for shells and multiple shells around a wide range of evolved objects, in order to quantify the total amount of mass lost at the various evolutionary stages of low to high-mass stars.
2. To study the dust and gas chemistry as a function of progenitor mass.
3. To study the properties and asymmetries of a representative sample of low- and intermediate- (i.e. AGB, post-AGB, PN) as well as high-mass (i.e. RSG, WR, LBV) post main sequence objects, and supernovae.

The list of Planetary Nebulae (PNe) in our sample is shown in Table 1. On this poster we present spectroscopy of the Helix nebula (NGC 7293) and imaging results of NGC 650. Imaging results for the Helix nebula will be discussed on a separate poster by Van de Steene et al.



Table 1: Overview of the PN observations that have been collected. Unless noted otherwise, all data are part of the proposal KPGET.mgroen01.1.

target	observing mode	date
NGC 650	PACS Phot.	2010-02-23
	SPIRE Phot.	2010-02-24
NGC 6302	PACS Spec.	2011-10-05
	SPIRE Spec.	2010-02-26
NGC 6537	PACS Spec.	2011-10-22
	SPIRE Spec.	2012-04-02 (GT2.mbarlow.1)
NGC 6543	PACS Phot.	2011-05-07
	SPIRE Phot.	2009-12-26
NGC 6720	PACS Phot.	2009-10-10 (SDP.mgroen01.3)
	SPIRE Phot.	2009-10-06 (SDP.mgroen01.3)
NGC 6853	PACS Phot.	2010-04-04
	SPIRE Phot.	2010-10-11
	PACS Spec.	2013-04-13 (OT2.pvanhoof.2)
	SPIRE Spec.	2013-04-16 (OT2.pvanhoof.2)
NGC 7027	PACS Phot.	2010-05-05
	SPIRE Spec.	2009-11-12
	SPIRE Spec.	2010-01-09
NGC 7293	PM Phot.	2010-04-28
	SPIRE Phot.	2012-12-08 (DDT.mustdo.7)
	SPIRE Spec.	2012-11-25 (DDT.mustdo.7)
	SPIRE Spec.	2012-12-17 (OT2.pvanhoof.2)

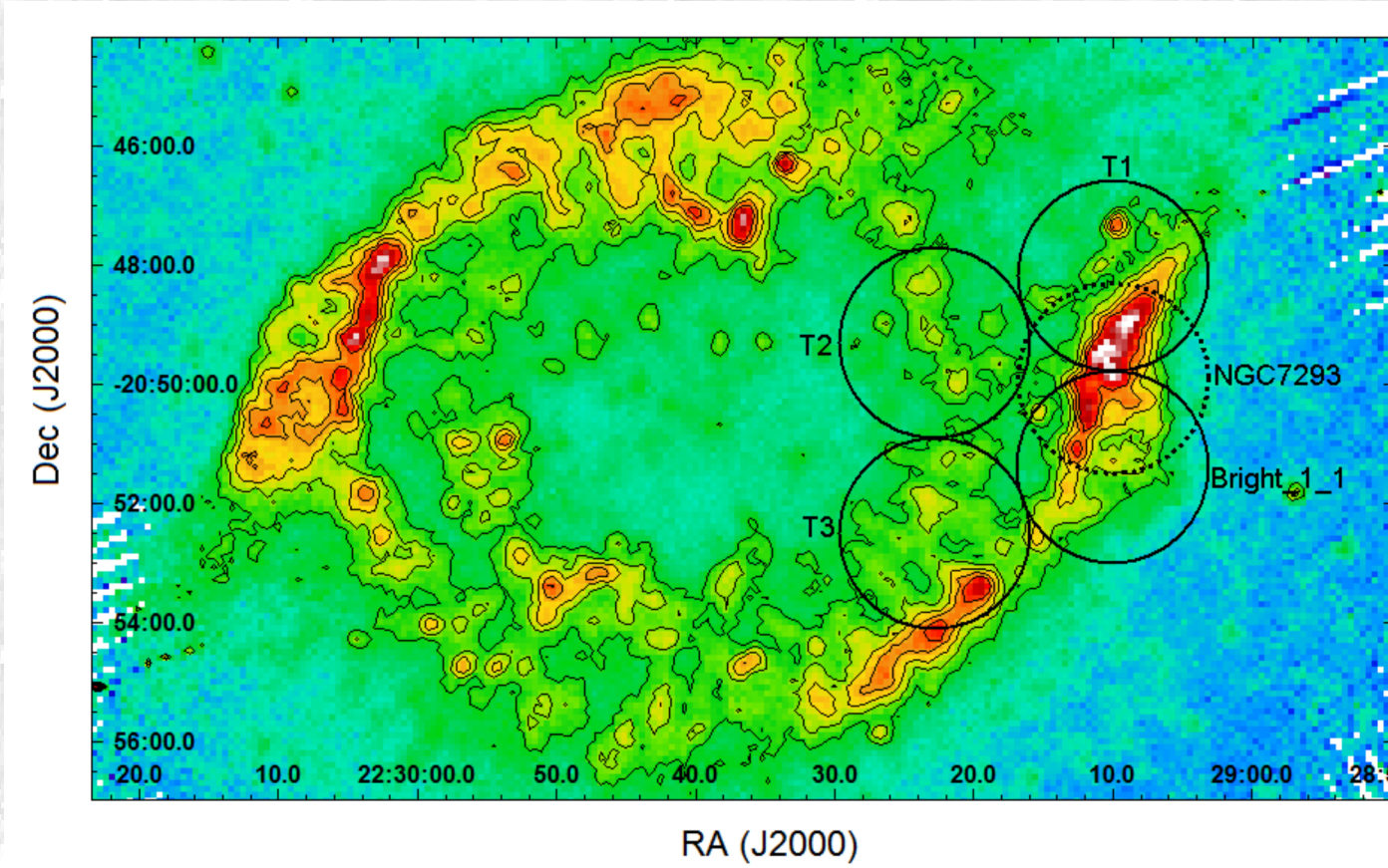


Figure 1 - Footprint of the SPIRE FTS pointings on the SPIRE 250 μm image. The solid circles show the positions of the MUSTO proposal and the dashed circle shows the position of the OT2 proposal.

2. Herschel spectroscopy of the Helix nebula

We combined the SPIRE spectra that we obtained in the DDT must-do and the OT2 proposal. The pointings for each of the observations are overlaid on the SPIRE 250 μm image in Fig. 1. The SPIRE image will be discussed further on a separate poster by Van de Steene et al.

The spectra cover the range 194 – 313 μm for SSW and 303 – 671 μm for SLW. In Fig. 2 we show the co-added SLW spectra over the inner and outer ring. They show detections of both [C I] lines, CO 4–3 through 7–6, and two OH⁺ N = 1–0 lines, as well as a tentative detection of the o-H₂O fundamental (not marked). The SSW spectra are not shown. They are clearly noisier and only contain detections of two OH⁺ lines (one of which is also visible in the SLW spectra) and the [N II] line at 205 μm.

The OH⁺ lines shown here constitute the first detection of OH⁺ emission in a planetary nebula. A map showing the distribution of the OH⁺ emission is shown in Fig. 3. In Fig. 4 we show composite images of the [N II], CO, OH⁺, and [C I] emission. They indicate that the OH⁺ and [C I] emission are strongly correlated. The CO emission largely comes from areas that also emit OH⁺ and [C I], though the CO emission seems more narrowly confined and is slightly shifted towards the central star. The [N II] emission clearly has a very different distribution from the molecular or [C I] emission.

The CO emission indicates a very low temperature between 20 and 40 K, in good agreement with the temperatures found by Zack & Ziurys (2013). The column density for CO is in the range $7\text{--}12 \times 10^{14} \text{ cm}^{-2}$. Assuming a fractional CO abundance of 2.2×10^{-4} (Bachiller et al. 1997), this yields a molecular hydrogen density of $2\text{--}6 \times 10^{11} \text{ cm}^{-3}$ if the H₂ formation is complete. A non-LTE radiative transfer model provides a kinetic gas temperature similar to the rotational temperature of CO and a molecular hydrogen density of $1\text{--}6 \times 10^9 \text{ cm}^{-3}$, in good agreement with the densities in the knots determined by Meaburn et al. (1998) and Huggins et al. (2002).

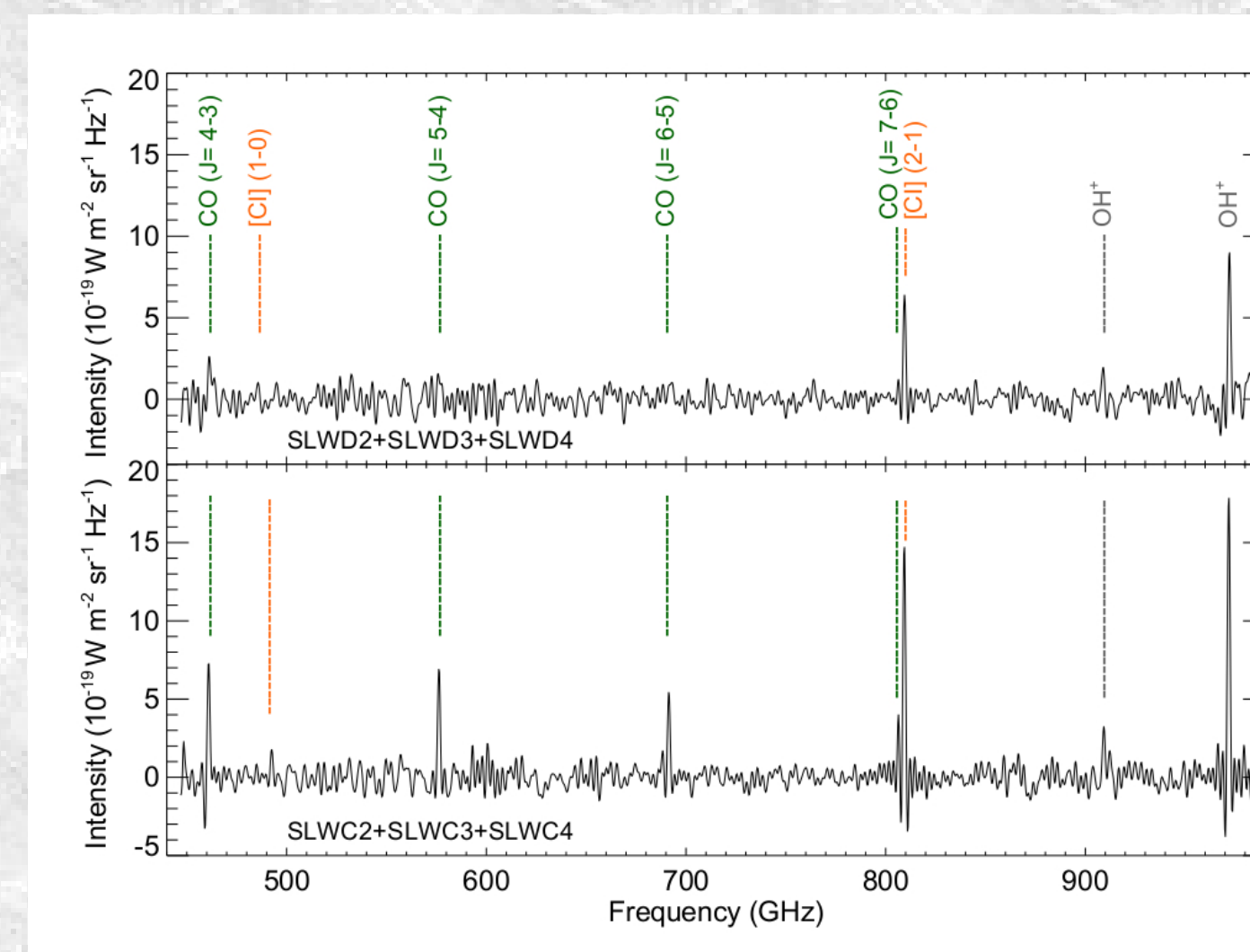


Figure 2 - Co-added spectra of three SLW detectors along the inner ring (top panel, positions T2 and T3) and along the outer ring (bottom panel, positions T1, Bright_1.1, and OT2).

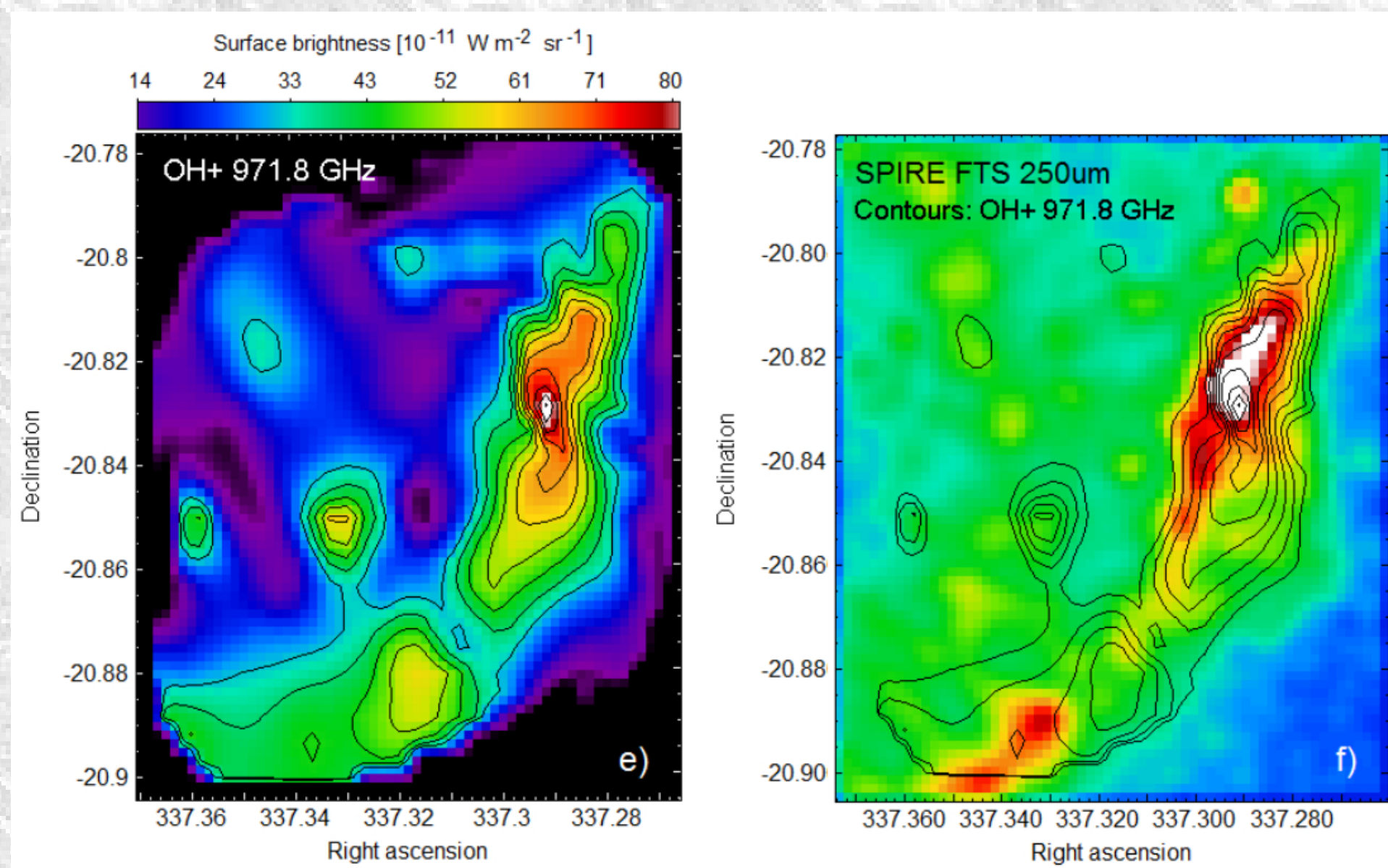


Figure 3 - Surface brightness map of the OH⁺ line at 971.8 GHz. In the right-hand panel, the contours of the OH⁺ emission are overlaid on the SPIRE 250 μm map.

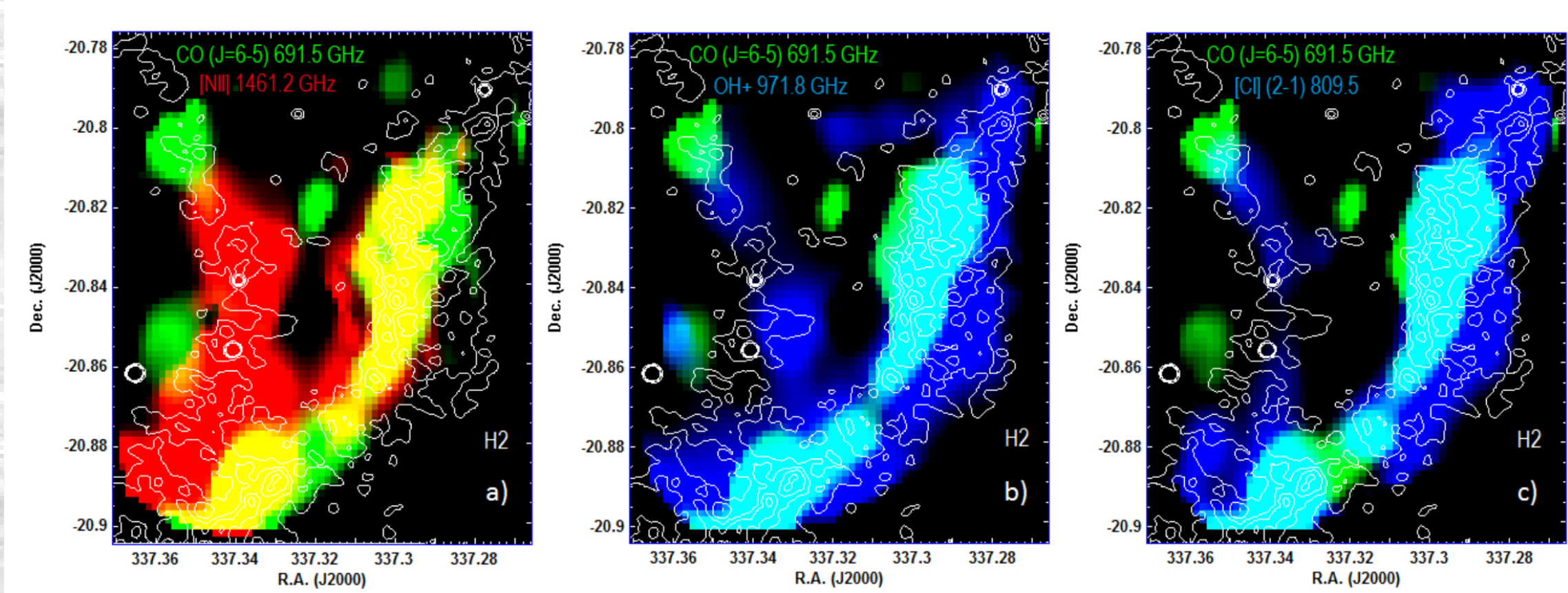


Figure 4 - Three composite images showing the distribution of different atoms, ions, and molecules along the rings of the Helix nebula.

3. Herschel observations of NGC 650

We used the Herschel PACS 70 and 160 μm images (shown in Figs. 5 and 6) to create a temperature map of the dust in NGC 650 (see Fig. 7). Additionally we created a photoionization model of the nebula using Cloudy C10.01, last described by Ferland et al. (1998). This model was used to interpret the Herschel data. Using this model we could establish that the central star is hotter than hitherto assumed: between 165 and 178 kK (or higher if there is more than $A_V = 0.1$ mag extinction towards the central star). The nebula is confirmed to be carbon-rich with C/O = 2.1.

We used the Herschel PACS & SPIRE photometry, in combination with IRAS and Spitzer data, to create a spectral energy distribution (SED) of the dust. This is shown in Fig. 8. We fitted a modified blackbody curve $F_\nu = C\nu^\beta B_\nu(T_{\text{dust}})$ to the data. The resulting fit parameters were $T_{\text{dust}} = 29.9 \pm 1.1$ K and $\beta = 2.12 \pm 0.12$.

Using the Cloudy model we could establish that the grains in the ionized region are fairly large. If we assume that they are single-sized (this is the simplest assumption we can make) they would have a radius of 0.15 μm. These large grains are most likely inherited from the AGB phase.

In Fig. 9 it is clear that the hottest dust grains (shown by the contours at 31.5 K and higher) are only present in the low-density area along the polar axis of the torus. The lower temperature contours (30.5 K and lower) on the other hand, are more or less spherical and are centered on the central star. This is evidence for two radiation components heating the grains, one of which is quickly absorbed away in higher density gas. This component is direct emission from the central star, while the second component (giving rise to the spherical contours) is diffuse emission from the ionized gas (mainly Ly α).

This nebula is very unusual in that it is highly evolved, yet still has a noticeable internal extinction. It shows evidence for a very clumpy structure in H₂ emission (Marquez-Lugo et al. 2013). It is clear that all the neutral and molecular material resides inside these dense clumps which are embedded in the ionized gas, and not in a PDR surrounding the ionized region as is the case in some young PNe (e.g., NGC 7027). This is reminiscent of the situation in the Helix and the Ring nebula (van Hoof et al. 2010 and references therein). Excess dust emission around 25 μm may indicate the presence of stochastically heated very small grains (possibly PAHs) inside these dense clumps, in addition to the large grains that are also present in the ionized region.

These results are discussed in more detail in van Hoof et al. (2013).

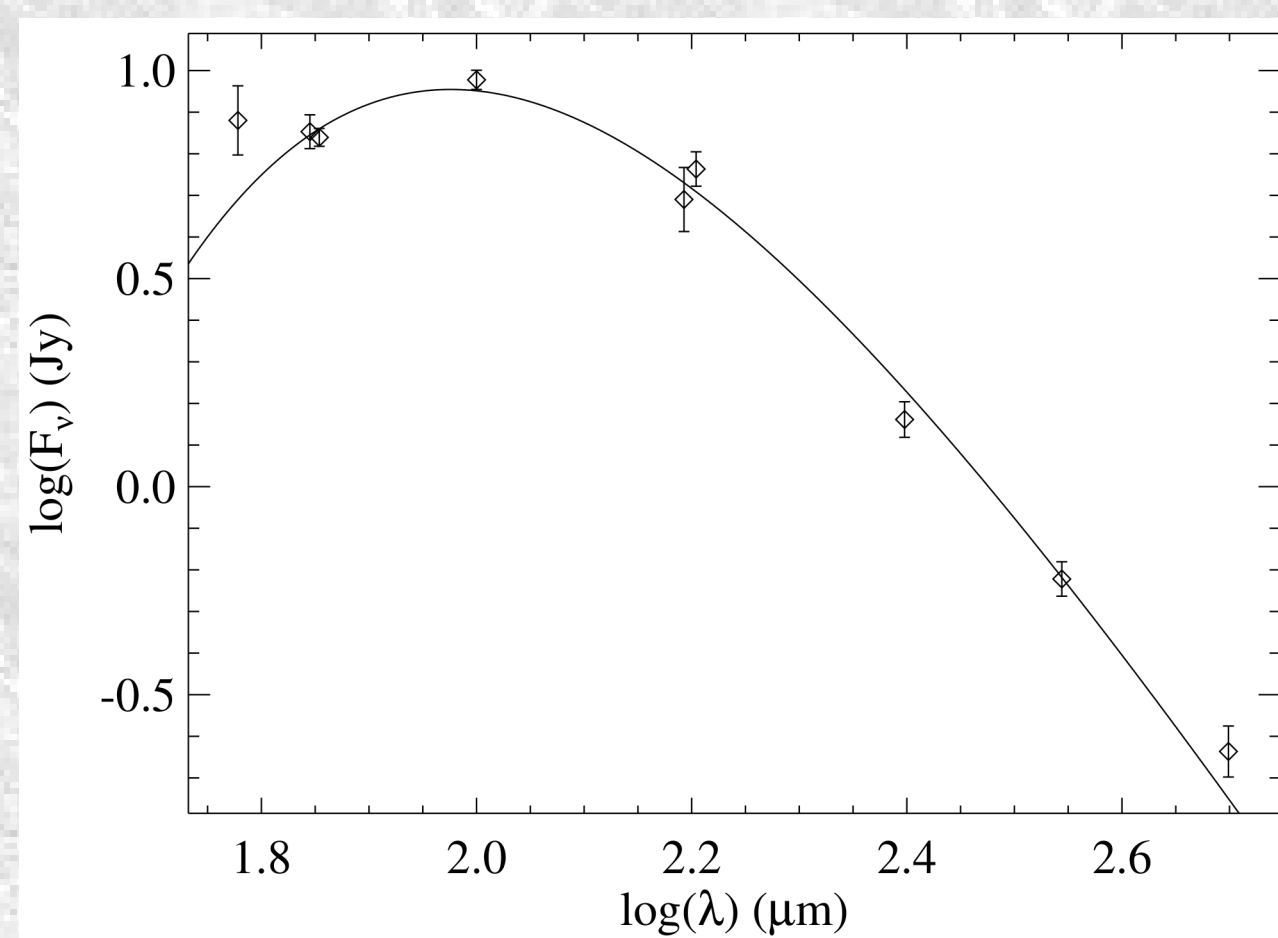


Figure 8 - The SED of the dust in NGC 650. The solid line shows the modified blackbody that was fitted to the observations.

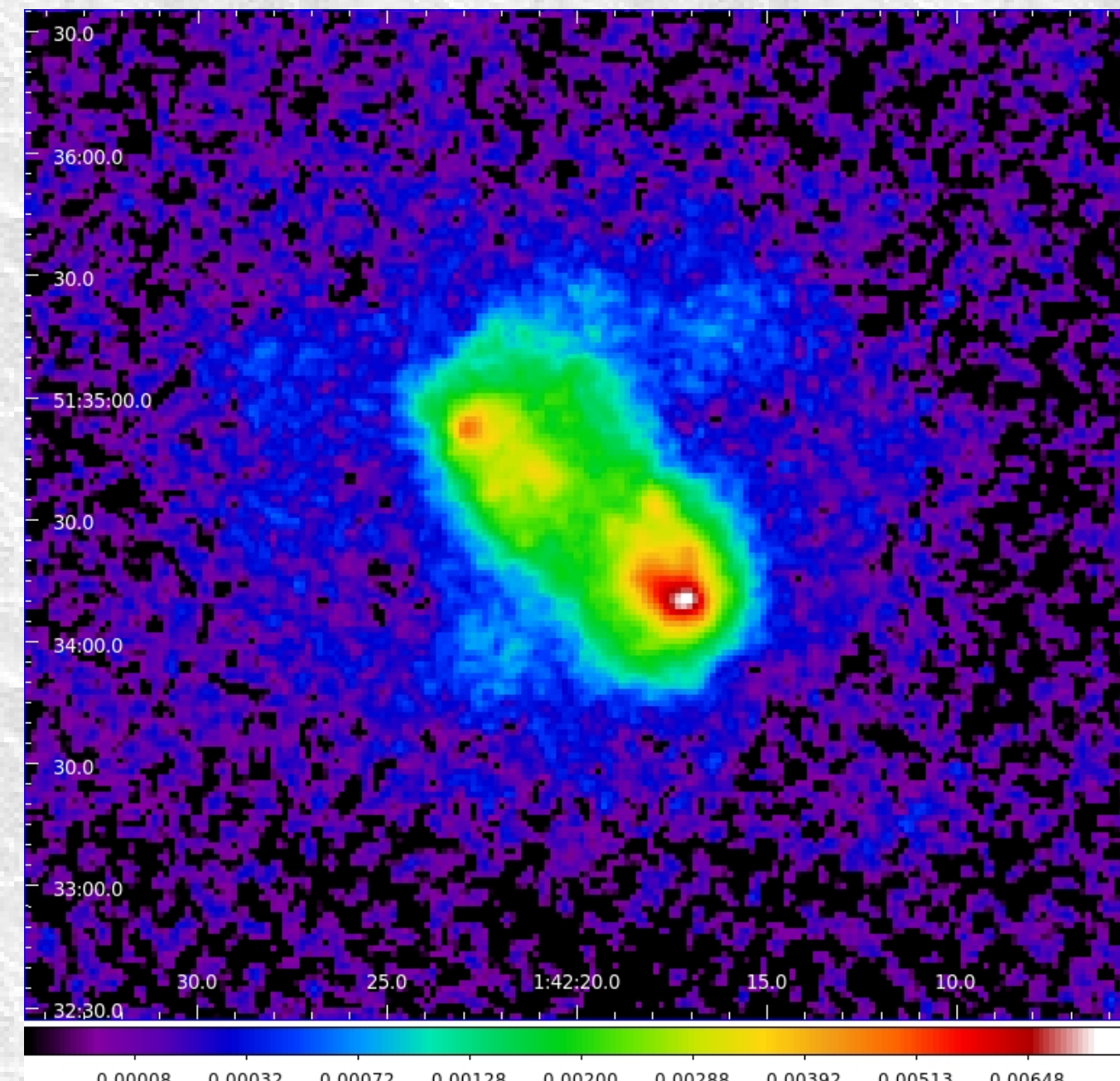


Figure 5 - The PACS 70 μm image of NGC 650 shown on a sqrt stretch. The color bar shows the flux density normalized in Jy/pixel.

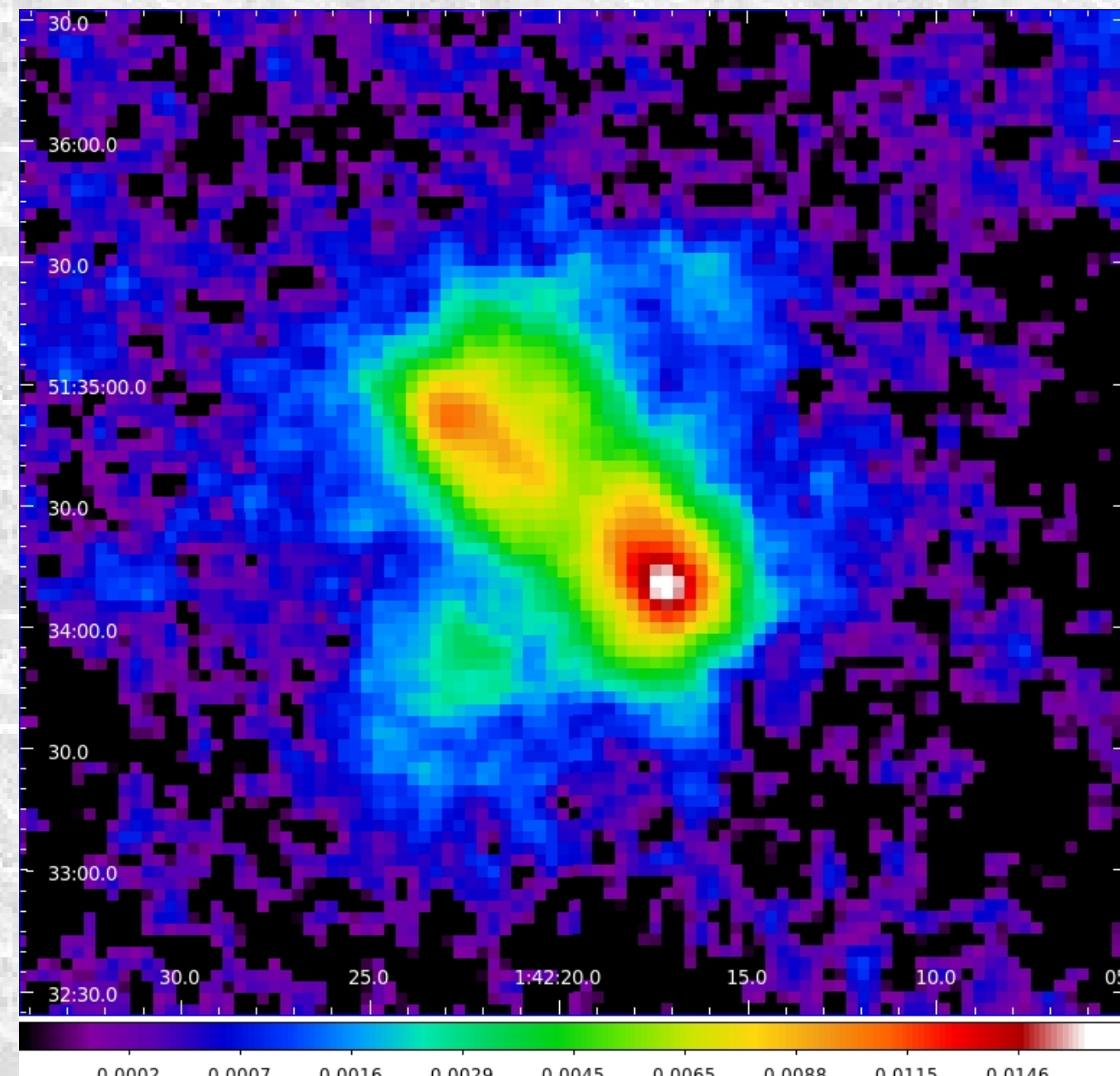


Figure 6 - Same as Fig. 5, but showing the PACS 160 μm image.

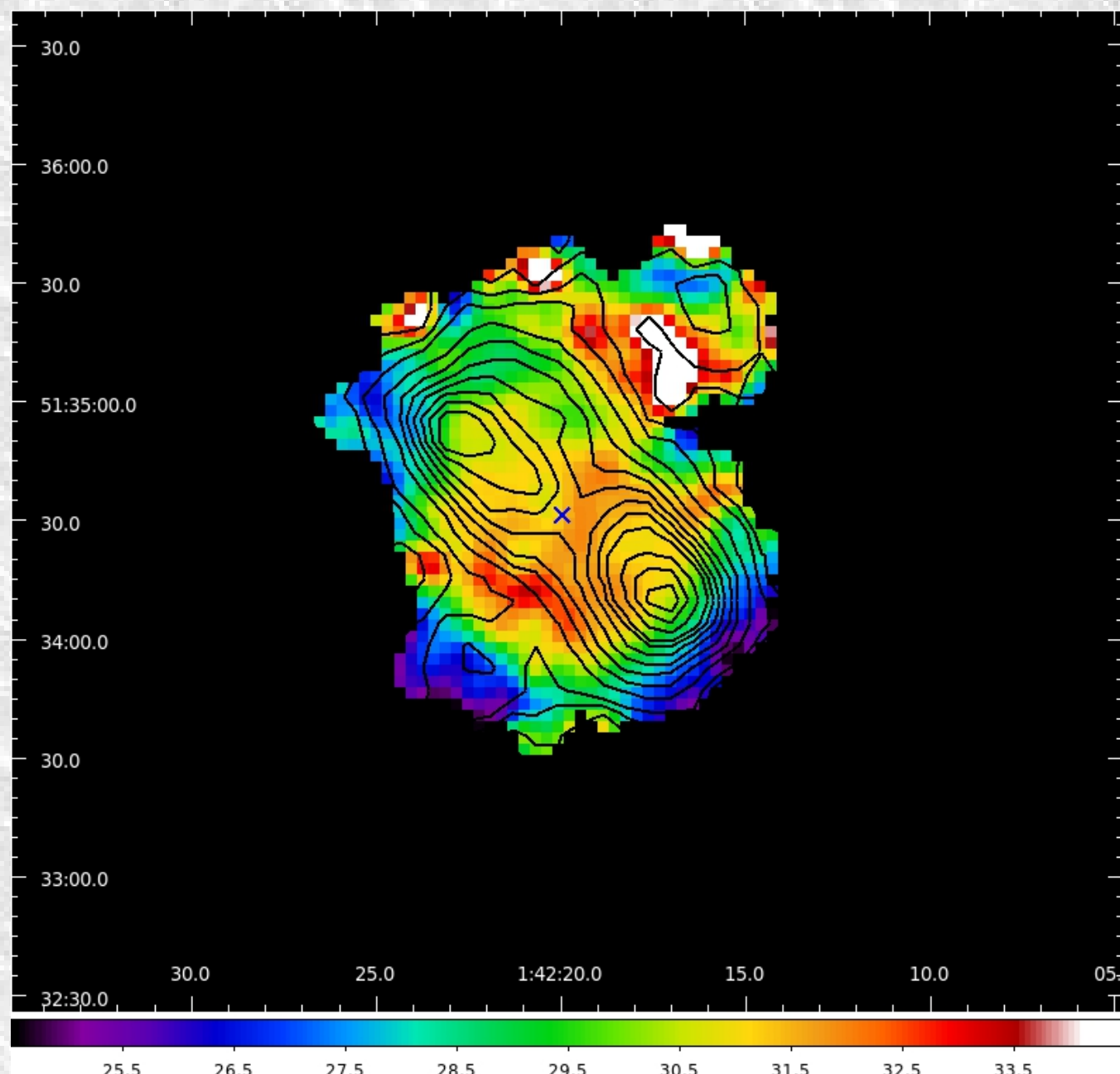


Figure 7 - The temperature map of NGC 650 created from the PACS 70 / 160 μm ratio image. The black contours are taken from the PACS 160 μm image. The blue cross marks the location of the central star. The bar at the bottom shows the temperature scale.

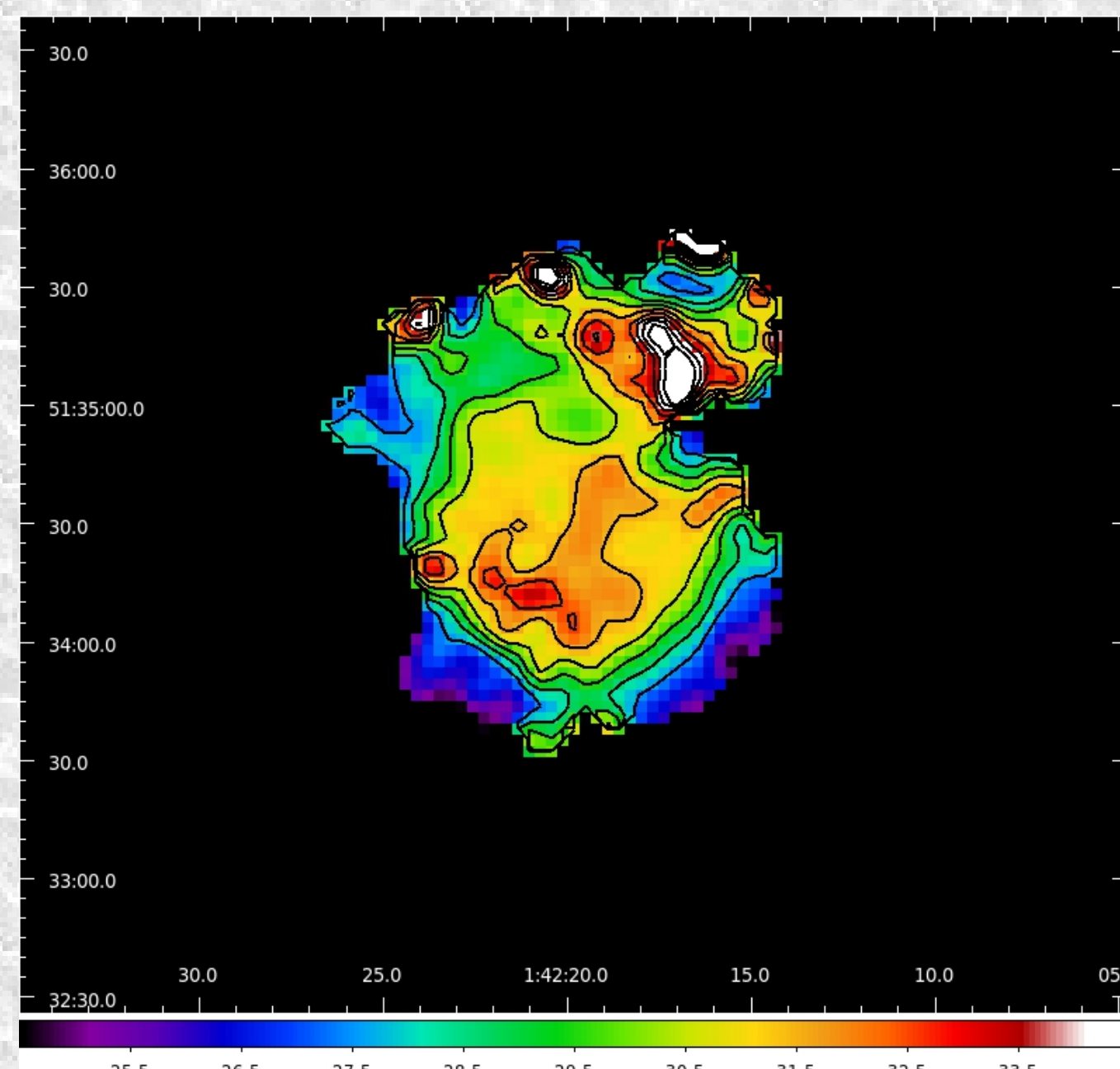


Figure 9 - Same as Fig. 7, but showing contours for the grain temperature. Contour levels are from 27.5 to 35.5 K with 1 K increments.

References

Bachiller R., Forveille T., Huggins P.J., Cox, P., 1997, A&A, 324, 1123
 Ferland G.J., Korista K.T., Verner D.A., et al., 1998, PASP, 110, 761
 Groenewegen M.A.T., Waalkens C., Barlow M.J., et al., 2011, A&A, 526, A162
 Huggins P.J., Forveille T., Bachiller R., et al., 2002, ApJ, 573, L55
 Marquez-Lugo R.A., Ramos-Larios G., Guerrero M.A., Vázquez R., 2013, MNRAS, 429, 973
 Meaburn J., Clayton C.A., Bryce M., et al., 1998, MNRAS, 294, 201
 van Hoof P.A.M., van de Steene G.C., Barlow M.J., et al., 2010, A&A, 518, L137
 van Hoof P.A.M., Van de Steene G.C., Exter K.M., et al., 2013, arXiv:1308.2477
 Zack L.N., Ziurys L.M., 2013, ApJ, 765, 112

